JCTC Journal of Chemical Theory and Computation

Adsorption of Ethylene, Vinyl, Acetic Acid, and Acetate Species on PdAu(111) and PdAu(100) Surface Alloys: A Cluster Model Study

Ivan Rivalta, Gloria Mazzone, Nino Russo, and Emilia Sicilia*

Dipartimento di Chimica and Centro di Calcolo ad Alte Prestazioni per Elaborazioni Parallele e Distribuite-Centro d'Eccellenza MURST, Università della Calabria, I-87030 Arcavacata di Rende, Italy

Received January 7, 2009

Abstract: The adsorption properties on PdAu surface alloys of ethylene and acetic acid molecules along with their derived vinyl and acetate surface species have been investigated by density functional theory calculations. Large clusters have been used to model second-neighbor Pd monomer pair ensembles on PdAu(100) and PdAu(111) surface alloys. Ethylene and acetic acid are weakly bonded to the Pd monomers, while vinyl and acetate are strongly bonded to both Pd and Au atoms being very stable surface species. The ligand effect of the gold atoms surrounding the Pd monomers has been shown to be stronger in the more dense PdAu(111) surface alloy. Cluster model results are in good agreement with experimental evidence providing important insight on the adsorption bonding modes, the assignment of the infrared features, and the preferred adsorption sites.

1. Introduction

Bimetallic systems constitute a broad class of selective catalysts that attempt to exploit and combine the different chemical properties of various metals toward a given chemical reaction.[1−4] Among the several binary systems that are often used in basic and applied research, PdAu provides an example of a rather versatile catalytic system. Mixtures of Pd and Au are frequently used as catalysts for a number of reactions (e.g., CO oxidation, cyclotrimerization of acetylene, synthesis of vinyl acetate monomer, selective oxidation of alcohols to aldehydes)[5−8] and applications including hydrogen fuel cells and pollution control.[9,10] It has been shown that the addition of Au to Pd significantly enhances the catalytic activity, selectivity, and stability of Pd-based catalysts; therefore, Pd−Au surface alloys have been the subject of many investigations.[6,7,11−18]

One of the major uses of gold/palladium catalysis is for vinyl acetate monomer (VAM) production. Indeed, the synthesis of vinyl acetate monomer from ethylene, acetic acid, and oxygen is catalyzed by both supported palladium and palladium−gold alloys, but alloying with gold leads to a substantial increase in selectivity.[19] Although this process is a mature industrial reaction, the nature of the key reaction intermediates and mechanism as well as the promotional role of Au are still unresolved questions. Two different surface reaction mechanisms, both invoking coupling of acetate and ethylenic species as the rate-limiting step, have been proposed for VAM synthesis. The one proposed by Samanos et al. involves the coupling of ethylene with adsorbed acetate to form, as intermediate, ethyl acetate that undergoes β-hydride elimination to form VAM (Samanos-type mechanism).[20] Alternatively, as suggested by both Moiseev[21,22] and Nakamura and Yasui,[23] ethylene could adsorb and subsequently dehydrogenate to form a vinyl species that couples with the coadsorbed acetate to give VAM directly (Moiseev-type mechanism). Although support to the pathway proposed by Samanos et al. comes from the experimental results by Tysoe et al. on Pd(111) surface,[24] the reaction mechanism for VAM synthesis remains essentially uncertain.

Goodman and co-workers[25] recently demonstrated that the critical ensemble for VAM formation on a PdAu(100) surface alloy is a pair of noncontiguous, suitably spaced, Pd monomers. They have also used ultra-high-vacuum (UHV)

* To whom correspondence should be addressed. E-mail: siciliae@unical.it.

10.1021/ct9000137 CCC: $40.75
Published on Web 04/20/2009

scanning tunnelling microscopy (STM) to image the Pd monomer pairs on AuPd(100) bulk alloy surface and presented a method for increasing the concentration of these active sites.[26]

The formation of isolated Pd monomer sites influences the properties of adsorbed reagents (ethylene, acetic acid, and their derived surface species) as well. Indeed, temperature-programmed desorption (TPD) experiments have shown that ethylene binds significantly less strongly to a Pd monomer compared to a site containing contiguous Pd atoms.[27,28] On contiguous Pd sites a di-σ-bonded ethylene species and an ethylidyne species have been observed,[29] which decompose leading to the formation of carbon, while on Pd monomers surrounded by gold atoms a π-ethylene surface species has been observed.[25,28,29] The addition of Au inhibits the decomposition of ethylene, consequently forming less carbon and extending the activity of the catalyst.[25] The same effect of gold addition to Pd surfaces has been demonstrated for the acetic acid and acetate decompositions.[30,31] High-resolution electron energy loss spectroscopy (HREELS) experiments[25,29] have shown the presence of a bidentate acetate species on isolated and contiguous Pd sites on PdAu(111) surfaces at high temperatures (350 K). By use of reflection−absorption infrared spectroscopy (RAIRS),[31] intact acetic acid molecules that form catemers have been detected for Au-rich PdAu(111) surface, whereas both bidentate and monodentate acetate species have been observed on surface alloys containing small mole fractions of gold. Recently, the effect on the adsorption of reactants (in VAM synthesis) has been demonstrated to be an important factor in determining the structure sensitivity of PdAu surface alloys.[32]

Since accurate knowledge of the binding sites and of the orientation of the molecules adsorbed on surfaces is an important component of any effort to describe heterogeneously catalyzed reactions with mechanistic detail, here we present the outcome of a density functional cluster model study of the adsorption properties of ethylene, vinyl, acetic acid, and acetate species on the PdAu(111) and PdAu(100) surface alloys. Ethylene and acetic acid (along with molecular oxygen) are the starting reagents in the VAM synthesis and the species that deposit from the gas phase on the catalyst surface. Their derived species, acetate and vinyl, are the most relevant surface species if both Samanos-type and Moiseev-type mechanisms are considered viable on PdAu surfaces.

The focus of the present paper is on the local features of the interaction between adsorbed molecules and PdAu surface alloys. Consequently, we adopted for our investigation the cluster model approach as more suitable, with respect to alternative slab models, to capture the essential features of the chemisorption bond and to predict local properties such as adsorption geometries and vibrational frequencies at low coverages. In particular, cluster models have been built up to represent the second-neighbor Pd pair ensembles on both surfaces given that these are the critical ensembles in the synthesis of vinyl-acetate monomer catalyzed by PdAu alloys and supposed to be crucial for the different catalytic activities of PdAu(100) and PdAu(111) surfaces.

Results have been compared with previous periodic slab supercell calculations for the PdAu(001) surface[33,34] and also with helpful information concerning the adsorption properties of acetic acid-derived species and ethylene on Au/Pd(111) alloys as a function of temperature and alloy composition comprised in a recent series of systematic experimental studies carried out by Tysoe's group.[11,28,31]

2. Methodology and Computational Details

In order to model the second-neighbor Pd pair ensembles on PdAu(100) and PdAu(111) surfaces we have built up cluster models of large size having 57 and 64 metal atoms, respectively, in order to prevent any indirect insaturation effect for the surface atoms directly involved in the adsorbate−surface bonds. A schematic representation of the Pd_2Au_n clusters used in this work is reported in Figure 1.

Since these models have been successfully adopted for the study of CO adsorption on the PdAu surface alloys, a more detailed description of the Pd_2Au_{55}(24,21,12) and Pd_2Au_{62}(30,21,13) cluster models used here along with the cluster size dependence of the chemisorption properties can be found elsewhere.[35] The employed clusters are three-layer models centered in the active site that contains two noncontiguous Pd atoms and two Au atoms bonded to both of them. The atomic positions of the clusters have been assigned, initially, as in bulk gold, with the experimental lattice parameter of 4.08 Å. For the adsorption studies, the positions of the molecules, adsorbed on these cluster models, have been fully relaxed without symmetry constraints. Cluster atoms involved in the adsorption bonds and their first neighbors in the first and second layers have been also relaxed. The calculations have been performed with the Turbomole package[36] at the DF level, by use of the BP86 functional[37,38] within the resolution of the identity approximation for computing the electronic Coulomb interaction (RI-J).[39,40] The Stuttgart effective core potential[41] has been used to model the scalar relativistic effects replacing the 28 and 60 core electrons of palladium and gold atoms, respectively. The valence electrons of metal atoms, 18 for Pd and 19 for Au, and all electrons for C, O, and H atoms have been explicitly considered by use of the Turbomole's TZVP basis set[42] along with the corresponding TZVP auxiliary basis set.[40] The electronic ground states of bare PdAu clusters and adsorbate/cluster models (including ionic adsorbates) have been checked by studying different spin multiplicities. The lowest energy states have always shown the smallest multiplicity values (i.e., singlet or doublet states). The total energies calculated after geometry optimization have been corrected for basis set superposition error (BSSE) by use of Boys−Bernardi counterpoise calculations[43] for all adsorbate/cluster models. This correction is less than 4.0 kcal/mol per bond for the strong chemisorption of acetate radical and vinyl species on the cluster models, whereas is around 1.0−1.3 kcal/mol for the weak adsorption of ethylene and acetic acid molecules. As expected, for the absorption of charged species, i.e., CH_3COO anion, the correction is larger up to ∼7−8 kcal/mol. All the vibrational frequencies reported in this work have been corrected by use of the scaling factor (1.004) suggested for the BP86 functional in combination

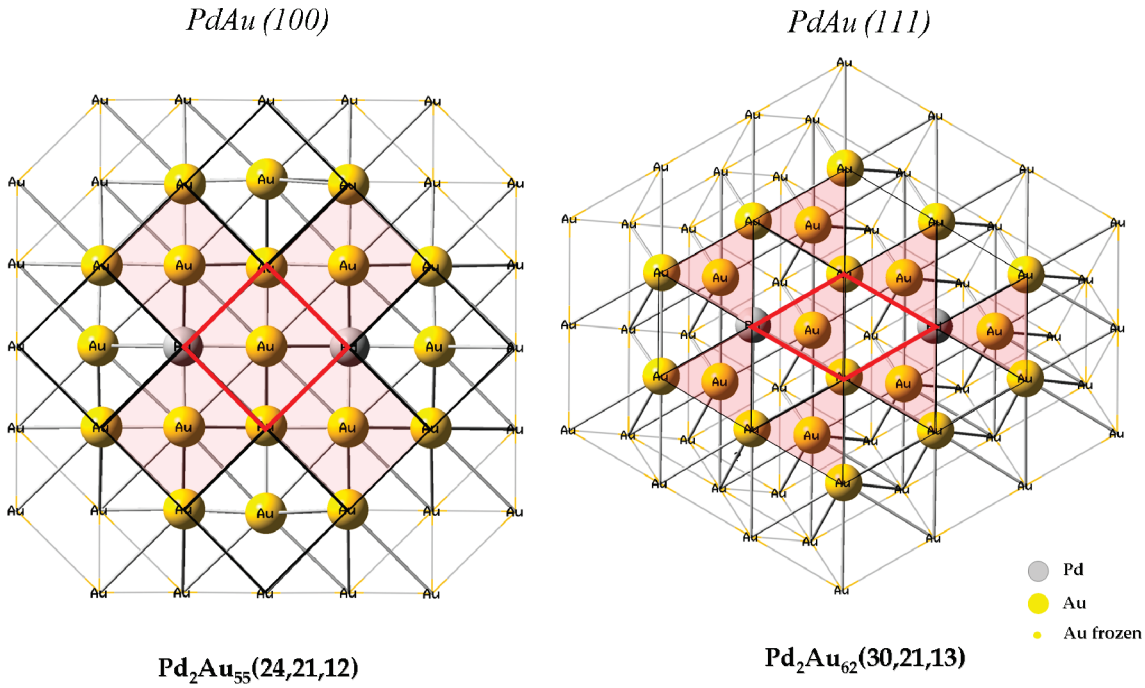

Figure 1. Schematic representation of the Pd_2Au_n clusters used in this work to model the second-neighbor Pd pair ensemble on the PdAu(100) and PdAu(111) surface alloys. Frozen Au atoms are shown as spots, while Pd and Au atoms in the first and second layer that are allowed to relax are depicted as spheres. Four-fold and three-fold (hcp) hollow sites associated with the relaxed atoms in the first layer are evidenced by planes (in red). Unit cells of the Au(100) and Au(111) pure surfaces are depicted in red.

with the TZVP basis set.[44] The atom-projected density of states (DOS) has been calculated (as implemented in Turbomole) by broadening the discrete energy levels of each cluster model with Gaussians having a width of 0.003 au and superimposing them.

3. Results and Discussion

3.1. Adsorption of Ethylene. Experimental studies by both Goodman's[25,29] and Tysoe's[28] groups have demonstrated that on gold−palladium alloys at low palladium coverages only π-bonded adsorbed ethylene on isolated Pd atoms, completely surrounded by gold, is present as surface species.

In accordance with this experimental evidence, the DF cluster model calculations performed in this study have shown that there are no stable adsorption states for a di-σ-bonded ethylene on second-neighbor Pd monomer pairs. Indeed, despite the numerous attempts to find on both PdAu(100) and PdAu(111) surface alloys a stable adsorption geometry having Pd−C and Au−C σ bonds, the ethylene molecule always moves to an atop configuration (π-bonded-type) on a Pd atom completely surrounded by gold.

The energetic, structural, and vibrational properties calculated for the π-bonded ethylene molecule adsorbed on top of Pd monomer are reported in Table 1 for both PdAu(100) and PdAu(111) palladium−gold surface alloys.

For the PdAu(100) surface, the calculated binding energy (BE) of ethylene is 13.0 kcal/mol, in good agreement with the values obtained by use of a plane-wave-based method[33] for isolated Pd monomers (12.9 kcal/mol) and second-neighbor Pd monomer pairs (15.2 kcal/mol). The geometry of the adsorbed ethylene molecule with the C−C bond along the [011] axis of the PdAu(100) surface is energetically preferred by only 0.7 kcal/mol with respect to that along the [010] axis, analogously to what has been obtained with the periodic slab supercell approach.[33]

Since the experimental BE of the π-bonded ethylene on the Pd(100) clean surface is ~19 kcal/mol[45] and this value

Table 1. BSSE-Corrected Binding Energies (BE, in kcal/mol), Equilibrium Bond Distances (*d*, in Angstroms), Angles (in degrees), and Scaled Vibrational Frequencies (in cm^{-1}) of the π-Bonded Ethylene Molecule on the Pd_2Au_{55}(24,21,12) and Pd_2Au_{62}(30,21,13) Cluster Models[a]

	PdAu(100)	PdAu(111)
BE	13.0	5.5
d(C−C)	1.383	1.374
d(Pd−C)	2.299	2.383
θ(CCH)	120.6	121.1
ϕ_{tilt}	8.4	5.1
ν(C−H)	3184 (w)	3178 (w)
	3159 (w)	3152 (w)
	3083 (w)	3083 (w)
	3080 (w)	3076 (w)
ν(C−C) + $\delta(CH_2)$	1530 (w)	1607 (w)
	1422 (w)	1430 (w)
	1276 (w)	1336 (w)
	1203 (w)	1206 (w)
$\omega(CH_2)$	958 (w)	1005 (w)
	922 (s)	938 (vs)
	900 (s)	925 (s)
	818 (w)	811 (w)
ν(Pd−C)	175 (w)	158 (w)

[a] The ϕ_{tilt} angle indicates the tilting angle between the ethylene molecular plane and the surface plane. ν stretching; δ in-plane bending, scissoring and rocking; ω out of plane bending, twisting and wagging. (vs) very strong; (s) strong; (w) weak.

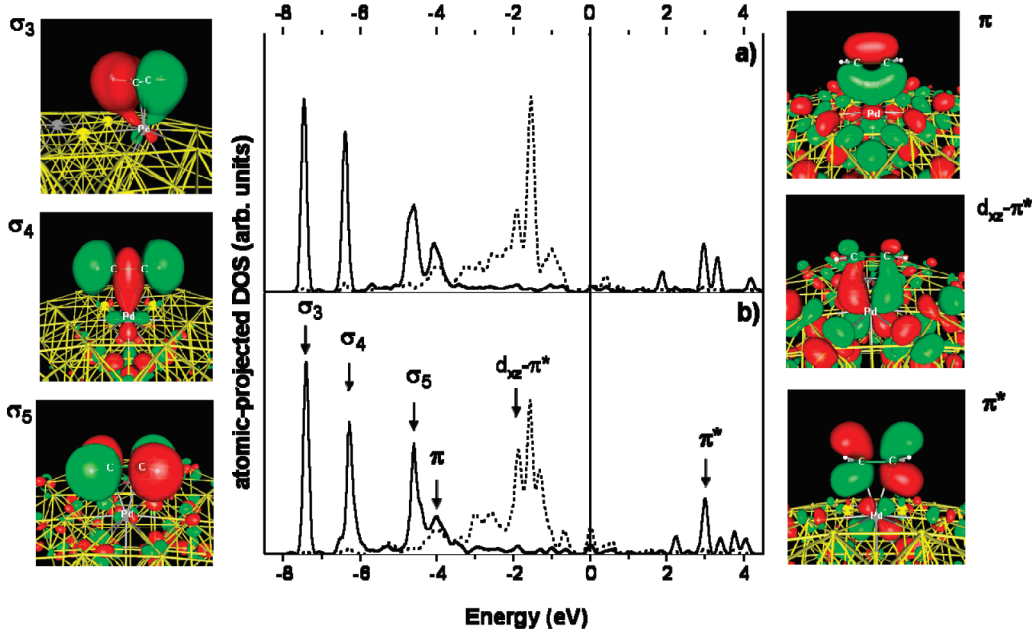

Figure 2. Atom-projected DOS of ethylene molecule (black lines) and Pd d states (dotted black lines) in the C_2H_4/Pd_2Au_{55} (a) and C_2H_4/Pd_2Au_{62} (b) systems. The insets display the full orbital character (contour factor 0.03) of the σ_3, σ_4, and σ_5 peaks (left) and π, π^*, and $d_{\pi z}-\pi^*$ bands (right) of the C_2H_4/Pd_2Au_{62} cluster model. The zero of energy indicates the highest occupied molecular orbital.

significantly decreases by gold addition due to the ligand effect,[33,34] the interaction of the π-bonded ethylene with Pd monomers finally is in the energy regime of the chemisorption/physisorption limit.

Unsurprisingly, this effect has been also observed for the adsorption of C_2H_4 on the PdAu(111) surface. The BE value for this adsorption, calculated with the cluster model used in this study, is 5.5 kcal/mol and is just a little lower than the calculated BEs for the Pd(111) surface, which are in the range of 6.4−7.2 kcal/mol.[45−47] These results are in line with the observations made in the TPD experiments on PdAu(111) surface alloy,[28] which indicated that the heat of adsorption of ethylene decreases monotonically as the gold coverage increases. On the other hand, a desorption activation energy of 13.6−14.8 kcal/mol has been estimated experimentally[28] for the ethylene adsorption on PdAu(111) with medium−high gold coverage (between ∼0.5 and ∼0.7). The computed BE is, therefore, underestimated by about 7−9 kcal/mol with respect to the experimental value. However, it is worth underlining that this discrepancy, beside the DFT limits in the description of such long-range interactions, can be due to the uncertainty associated with the experimental estimation of the heat of adsorption. Indeed, peak broadness, in the TPD spectra, is observed for the ethylene adsorption on PdAu(111) surface at gold coverage higher than 0.73 ML. Furthermore, the stronger interaction between ethylene and the PdAu(100) surface with respect to the PdAu(111) surface is in line with the behavior observed for the adsorption of other organic molecules (such as CO[45,48] and other adsorbed species studied here) on these two surfaces alloys.

The different adsorption orientations for the π-bonded ethylene on the PdAu(111) surface (i.e., with the carbon−carbon axis along the $0\bar{1}0$, $\bar{1}01$, and $\bar{2}11$directions) explored in this study have practically shown the same energetics, proving to be adsorption degenerate states.

The main infrared features of π-bonded ethylene have been detected in the range between 900 and 960 cm^{-1} by both RAIRS[28] and HREELS[25,29] experiments and assigned to the CH_2 wagging modes. In the same spectral region we found the most intense infrared vibrations that just correspond to the in-phase wagging vibrational mode, where in phase indicates the simultaneous wagging of the two CH_2 groups out of the molecular plane. In particular, in the case of the PdAu(111) surface alloys the main infrared feature (with the highest peak intensity, see Table 1) is calculated to lie at 938 cm^{-1}. This value is in excellent agreement with the main experimental feature detected at 931 cm^{-1} by RAIRS[28] for the π-bonded ethylene adsorbed on a PdAu(111) surface with a 0.73 ML gold coverage and annealed to 120 K (to prevent the interference of ethylene molecules adsorbed on Au atoms).

Further remarks regarding the analysis of the π-bonded ethylene vibrational spectra will be given in the next paragraph for a comparison with the calculated vibrational properties of the surface vinyl species.

The fundamental features of ethylene π-bonded adsorption on the Pd noncontiguous pairs can be described in the framework of the classic Dewar−Chatt−Duncanson model of orbital interactions.[49,50] The filled bonding π orbital of ethylene transfers charge to the empty metal d states at the surface, while the occupied metal d band back-donates electron density into the ethylene antibonding π^* orbital. This model is confirmed by our calculations, in agreement with the periodic slab supercell-projected DOS,[33] as shown by the atom-projected DOS for the C_2H_4/Pd_2Au_{55} and the C_2H_4/Pd_2Au_{62} cluster models depicted in Figure 2a and 2b.

In the noninteracting system (where the ethylene molecule is located 4 Å above the substrate) the highest occupied molecular orbital (HOMO) of ethylene and the lowest unoccupied molecular orbital (LUMO) lie at −1.2 and 3.9 eV, respectively. In the equilibrium structure of adsorbed ethylene on PdAu clusters, a relevant depletion of the π-orbital peak of ethylene (HOMO) can be observed at −4.0 eV along with a broadening of the π^* peak (LUMO) into a wide energy range, in accordance with the common donation and back-donation picture (see Figure 2). In general, small bonding and antibonding overlaps between Pd d bands and σ and π states of ethylene have been detected, in line with a Dewar−Chatt−Duncanson description of a weak chemical interaction. The main contribution to the adsorption bond comes from the coupling of the HOMO of ethylene with the empty d_{z^2} orbital of the Pd monomer.

As confirmed by the orbital plot at −2.0 eV ($d_{xz}-\pi^*$), some orbital states with π^* character appear to be occupied, but the feeble overlapping with the metal d states indicates a back-donation mechanism with a limited charge transfer.

According to this description of the Pd−ethylene interaction, a very small elongation of the C−C bond by 0.05 and 0.04 Å with respect to the gas-phase ethylene (1.333 Å) has been observed (see Table 1) on the PdAu(100) and PdAu(111) surfaces, respectively. The calculated Pd−C distances (about 2.3−2.4 Å) and the planar and tilt angles (θ and ϕ, respectively), whose values confirm a negligible distortion of the sp^2 hybridization of the C atoms, confirm the weak chemical interaction between ethylene and Pd atoms in the gold-rich PdAu surface alloys.

3.2. Adsorption of Vinyl. According to the Moiseev-type mechanism[21−23] the vinyl acetate formation involves a surface vinyl species that couples with the coadsorbed acetate. This radical species is a surface intermediate of the dehydrogenation reaction of an adsorbed ethylene molecule. However, it has been generally observed that ethylene decomposition leads to the formation of the stable surface intermediate ethylidyne on the close-packed fcc (111) and hcp (0001) metal surfaces,[51,52] while adsorbed vinylic (vinyl or vinylidene) species seem to be more favorable intermediates only on the more open fcc (100) surfaces.[51−54] On the other hand, the density functional study of the ethylene dehydrogenation pathways over Pd(111)[55] has strongly suggested that the surface vinyl species is even formed on this closed packed surface, but it is unlikely to be detected spectroscopically because it quickly reacts along other surface reaction paths (e.g., rehydrogenation of ethylene or ethylidyne formation[56]). These theoretical results are corroborated by low-energy electron diffraction (LEED) analysis of ethylene decomposition over Pd(111) at low temperature,[57] which suggests the presence of ∼15% of tilted species in the surface layer having the same geometry of a di-σ ($\eta^1\eta^2$) vinyl surface species.

The surface vinyl species formation from adsorbed ethylene, instead, seems to be inhibited over PdAu(001) surface alloys due to the high activation barrier of this elementary step, as recently suggested by slab supercell calculations.[33] It is worthwhile underlining that surface oxygen and hydroxyl groups should be present in the reaction conditions of VAM synthesis[25] leading to water formation. Since surface oxygen atoms promote the β-hydrogen elimination from ethyl acetate-like species (in the Samanos-type mechanism), lowering the activation barrier,[34] these surface species should also facilitate the formation of surface vinyl species by hydrogen abstraction from ethylene (in the Moiseev-type mechanism). Therefore, the theoretical predictions on the adsorption properties of vinyl radical on PdAu surface alloys are not meaningless and have been carefully carried out in this study in order to be possibly compared with future experimental studies.

On the clean Pd(111) surface the vinyl species prefers to adsorb with an $\eta^1\eta^2$(C,C) fashion, showing an approximate sp^3 hybridization at each C atom with a BE of 56−61 kcal/mol, whereas the η^1-atop adsorption mode (sp^2) is less favorable by about 10 kcal/mol, as indicated by both periodic slab and cluster model calculations.[55] All attempts to find local minima related to the $\eta^1\eta^2$ adsorption mode of vinyl on the cluster models of PdAu(100) and PdAu(111) surfaces have been unsuccessful, indicating that the absence of contiguous Pd monomers determines the destabilization of such an $\eta^1\eta^2$ (C,C) adsorption.

The most stable adsorption mode of vinyl on second-neighbor Pd monomer pairs is the σ-bonded η^1-vinyl on top of Pd monomer (denoted as η^1-Pd) with the vinyl molecule vertically adsorbed. The full geometry optimizations starting from the η^1-bridge and η^1-hollow adsorption modes relax to the η^1-atop one. Besides, a stable η^1-vinyl species adsorbed on top of the Au atom (denoted as η^1-Au) has been obtained on both the PdAu(100) and PdAu(111) surfaces having an adsorption energy 10−11 kcal/mol lower than the η^1-Pd vinyl species.

The vinyl radical adsorption properties on the Pd monomers and the Au atoms of both Pd_2Au_{55} and Pd_2Au_{62} cluster models in the stable η^1-atop configurations are listed in Table 2.

For the η^1-atop adsorption mode, all the orientations of the C−C axis with respect to the surface directions have shown the same adsorption energy. The BEs for the η^1-Pd vinyl on PdAu(100) and PdAu(111) surfaces alloys are 44.1 and 41.4 kcal/mol, respectively. These values are slightly lower than the calculated value of 49.5 kcal/mol for the same adsorption mode on the Pd(111) clean surface.[55] Therefore, even if the ligand effect of gold weakens the interaction between the Pd atom and the adsorbed vinyl, this radical species remains strongly bonded to the surface alloys. The C−C bond distance in the adsorbed vinyl species is, in fact, elongated with respect to the gas-phase vinyl molecule (1.309 Å), becoming similar to that of the gas-phase ethylene (1.333 Å). The sp^2 hybridization of both the C atoms in the surface vinyl species is also revealed by the θ(PdCC) angle, whose values (around 127°) are close to the 120° of ethylene. The small values of the tilting angle ϕ_{tilt} (between 2° and 7°) confirm the planarity of the Pd−vinyl system, which always is perpendicular to the surface plane.

Due to the loss of symmetry by the presence of the Pd−C bond instead of the H−C bond and to the different adsorption modes of the ethylene and vinyl surface species, the calculated vibrational spectra for the η^1-vinyl adsorbed

Table 2. BSSE-Corrected Binding Energies (BE, in kcal/mol), Equilibrium Bond Distances (*d*, in Angstroms), Angles (θ and ϕ, in degrees), and Scaled Vibrational Frequencies (in cm^{-1}) of the η^1-Pd and η^1-Au Vinyl Surface Species on the Pd_2Au_{55}(24,21,12) and Pd_2Au_{62}(30,21,13) Cluster Models[a]

	PdAu(100)		PdAu(111)	
	η^1-Pd	η^1-Au	η^1-Pd	η^1-Au
BE	44.1	34.6	41.4	30.3
d(C−C)	1.336	1.331	1.333	1.338
d(S−C)	2.007	2.071	2.016	2.113
θ(SCC)	127.7	125.7	127.5	125.5
ϕ_{tilt}	6.9	2.3	1.6	7.8
$\nu(CH_2)$asymm + ν(CH)	3126(w)	3149(w)	3124(w)	3128(w)
$\nu(CH_2)$symm + $\nu(CH)_{in}$	3099(w)	3119(w)	3090(w)	3114(w)
$\nu(CH_2)$symm + $\nu(CH)_{out}$	3026(w)	3040(w)	3027(w)	3030(w)
ν(CC)	1561(s)	1580(s)	1560(s)	1551(s)
(CH_2) sciss	1356(m)	1366(m)	1352(m)	1361(m)
CH_2CH $rock_{in}$	1154(vs)	1174(vs)	1145(vs)	1177(vs)
CH_2CH $rock_{out}$	929(w)	948(w)	909(w)	954(w)
CH_2CH wag_{in}	905(m)	938(m)	901(m)	952(m)
CH_2CH wag_{out}	842(w)	877(w)	841(w)	895(w)
ν(S−C)	443(w)	475(w)	449(w)	437(w)

[a] The ϕ_{tilt} angle indicates the tilting angle between the vinyl molecular plane and the plane normal to the surface. S indicates the surface atom involved in the adsorption bond (Pd for η^1-Pd and Au for η^1-Au). ν: stretching. Subscript in and out indicate the in-phase and out-of-phase motions of the CH_2 and CH groups. (vs) very strong; (s) strong; (m) medium; (w) weak.

molecule are, obviously, different with respect to those calculated for the π-bonded adsorbed ethylene (compare Table 1 with Table 2). In particular, the main infrared feature for the η^1-Pd vinyl is calculated at 1154 and 1145 cm^{-1} on PdAu(100) and PdAu(111), respectively, and is associated with the in-phase rocking vibration of CH_2 and CH groups, whereas, as already discussed, the main peak of the π-bonded ethylene on the two surface alloys corresponds to the in-phase wagging of CH_2 groups and lies at 922 and 938 cm^{-1}, respectively.

For both PdAu surface alloys, a significant red shift of the vinyl vibration features with respect to the ethylene-adsorbed case has been observed in all regions of the calculated spectra. The C−C stretching and in-plane CH_2 bending modes are largely coupled in a wide-frequency range (1203−1607 cm^{-1}) for the π ethylene, whereas they are red shifted in the range 929−1561 cm^{-1} and become less coupled in the vibrational spectra of the adsorbed vinyl. Furthermore, the C−C stretching mode at about 1560 cm^{-1} appears to be particularly intense in the calculated vibrational spectra of surface vinyl species and should be clearly visible experimentally. The stretching modes of C−H bonds and the out-of-plane bending modes are generally red shifted by 50−100 cm^{-1}. The former modes move from 3080−3184 cm^{-1} in the π-bonded ethylene to 3026−3126 cm^{-1} in the η^1-Pd vinyl, whereas the latter ones move from 841−905 to 811−1005 cm^{-1}. The most consistent red shift has been observed for the Pd−C stretching and moves from 158−175 cm^{-1} for the weak π interaction of ethylene with Pd monomer to 443−449 cm^{-1} for the strong σ bond involved in the Pd−vinyl interaction.

Very similar adsorption geometries have been obtained for the η^1-vinyl adsorbed on Au atoms, as it is shown in Table 2. The main difference in the calculated vibrational spectra concerns a blue shift by 20−30 cm^{-1}, which should be experimentally detectable in the case of the most intense vibrational frequency.

3.3. Adsorption of Acetic Acid. Experimental studies have shown that acetic acid adsorbs molecularly on Pd(111) surfaces and forms η^2-acetate species on heating, even if the formation of η^1-acetate species has not been excluded.[58] In this section we focus on the adsorption of acetic acid molecules on PdAu surface alloys by comparing theoretical results and experimental data.

Indications on the adsorption features of intact acetic acid molecules on PdAu(111) come from RAIRS experiments combined with TPD data.[31] One of the main conclusions of the combined TPD and RAIRS experiments, carried out as a function of gold content, is that acetic acid adsorbs molecularly and desorbs intact for gold mole fractions greater than ∼0.5. TPD spectra collected as a function of gold coverage show that the presence of gold does not change significantly the desorption activation energy (at about 200 K) of the acetic acid intact molecules. Indeed, the acetic acid desorption from the monolayer on Pd-rich PdAu(111) surface[31] and clean Pd(111)[58] and Pd(100)[59] surfaces occurs at about 200 K corresponding to a desorption activation energy of about 12 kcal/mol.

The BE for a di-σ-(O,O)-bonded acetic acid molecule on bridge sites of Pd(111) surface, calculated by use of both cluster and periodic slab supercell models, is in the range of 4.8−6.0 kcal/mol[60] and underestimated with respect to the experimental desorption activation energy.[58] On both Pd and PdAu the predominant form of surface acetic acid species is surface catemers, and the nature of the catemer is gold coverage dependent.[31,58] Since in the theoretical models, both here and in previous studies on Pd surfaces,[60] only the monomeric acetic acid species have been considered, a perfect agreement between the theoretical and experimental results is unlikely.

The acetic acid molecule can adsorb on Pd surfaces in both monodentate and bidentate ways, but periodic slab model calculations[60] have indicated that the bidentate η^2-(O,O) surface species is more stable with respect to the monodentate η^1-(O_C) one (where O_C indicates the carbonyl oxygen atom involved in the Pd−O bond) on the Pd(111) surface.

In our study all possible adsorption geometries of acetic acid on second-neighbor Pd monomer pairs have been considered (see Figure 3). In particular, both the η^2-(O,O) atop (Pd-chelating) and the μ_2-η^2-(O,O) bridge (Pd−Au, not chelating) bidentate adsorption modes have been examined. All attempts to find stable adsorption states having these geometries have been unsuccessful, indicating that bidentate adsorption of acetic acid monomer on isolated Pd sites is really improbable. Moreover, the possibility to find a μ_2-η^2-(O,O)-CH_3COOH bonded to both second-neighbor Pd monomers can be excluded due to the too long Pd−Pd distance in these ensembles (at least 4.08 Å) with respect to the O−O distance in the acetic acid molecule (2.270 Å). All the η^2-CH_3COOH adsorption modes force the adsorbate to obtain its high-energy isomeric configuration (the cis conformer).

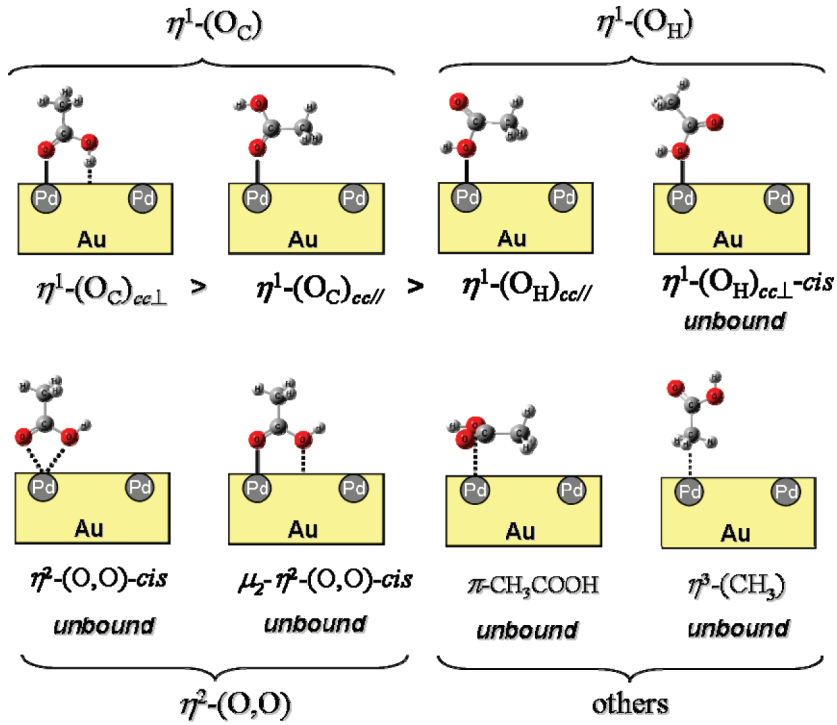

Figure 3. Adsorption geometries of acetic acid on second-neighbor Pd monomer pairs considered in this study. The stability trend on the PdAu surface alloys has been indicated. O_H and O_C specify the oxygen atom involved in the Pd−O bond in the monodentate adsorption, hydroxyl oxygen atom, and the carbonyl oxygen, respectively. The label *cis* indicates the less stable acetic acid conformer; *trans* is omitted.

Table 3. BSSE-Corrected Binding Energies (BE, in kcal/mol), Equilibrium Bond Distances (d, in Angstroms), Angles (θ, in degrees), and Scaled Vibrational Frequencies (in cm^{-1}) of the η^1 Adsorption Modes of Acetic Acid on the Pd_2Au_{55}(24,21,12) and Pd_2Au_{62}(30,21,13) Cluster Models[a]

			PdAu(100)			PdAu(111)		
	gas-phase CH_3COOH	exp[b]	η^1-$(O_C)_{cc\perp}$	η^1-$(O_C)_{cdl}$	η^1-$(O_H)_{cdl}$	η^1-$(O_C)_{cc\perp}$	η^1-$(O_C)_{cdl}$	η^1-$(O_H)_{cdl}$
BE		~12.0	9.0	5.1	2.9	5.6	3.0	2.1
d(Pd−O_C)			2.330	2.374		2.451	2.475	
d(Pd−O_H)					2.549			2.806
d(O−H)	0.980		1.011	0.991	0.988	1.010	0.990	0.990
d(H−S)			1.930		2.510	2.090		2.691
d(C−C)	1.513		1.508	1.501	1.504	1.510	1.504	1.509
d(C−O_C)	1.215		1.239	1.232	1.210	1.233	1.229	1.213
d(C−O_H)	1.365		1.332	1.346	1.388	1.338	1.350	1.376
θ(COH)	105.6		109.6	106.9	106.7	109.1	106.8	107.6
ν(O−H)	3622(m)		3243(vs)	3607(m)	3612(m)	3250(vs)	3611(m)	3607(m)
ν(C=O)	1820(s)	1720 (s)	1677(vs)	1714(vs)	1829(s)	1697(vs)	1727(vs)	1817(s)
$\delta_s(CH_3)$	1422(m), 1415(m)	1426 (br)	1420(w), 1410(m)	1435(m), 1415(m)	1412(m), 1402(m)	1422(w), 1411(m)	1431(m), 1413(m)	1422(m), 1414(m)
ν(C−O)	1371(m), 1309(m)	1294 (br)	1389(s), 1327(w)	1359(s), 1328(m)	1356(m), 1267(m)	1377(s), 1322(w)	1359(s), 1321(m)	1361(m), 1278(m)
γ(OH)	1184(s)	923/958 (s)	1201(m)	1199(s)	1151(s)	1199(m)	1197(s)	1148(s)
$\rho(CH_3)$	1035(m)	1052 (m)	1031(w)	1032(w)	1027(w)	1030(w)	1031(w)	1032(w)

[a] Geometrical parameters and vibrational frequencies for the free acetic acid molecule and available experimental data on PdAu(111) are reported for comparison. [b] Reference 31. ν, stretching; δ, deformation; γ, bending; ρ, rocking modes. For detailed assignments, see ref 61. (vs) very strong; (s) strong; (m) medium; (w) weak; (br) broad.

On the other hand, three monodentate adsorption modes are local minima having different stability on second-neighbor Pd monomer pairs. The adsorption properties of these monodentate acetic acid molecules are listed in Table 3.

Other explored adsorption geometries, such as those with the acetic acid molecular plane parallel to the surface or the methyl group forming a surface bond, are very unstable on the surface alloys studied here (Figure 3).

The monodentate CH_3COOH can bond to the Pd monomers through the hydroxyl oxygen atom (O_H) or the carbonyl oxygen (O_C). On both PdAu(100) and PdAu(111), the η^1-(O_C)-CH_3COOH geometry is more stable than the η^1-(O_H)-CH_3COOH (see Figure 3).

In particular, the η^1-(O_C)-CH_3COOH having the C−C axis perpendicular to the surface plane (denoted as η^1-$(O_C)_{cc\perp}$) is the most stable adsorption state and shows BE values of 5.6

and 9.0 kcal/mol on the PdAu(111) and (100) surfaces, respectively.

In this adsorption geometry the O−H bond points to the hollow site of the surface, forming a very weak hydrogen bond with the gold surface that to some extent stabilizes this adsorption state. The O−H bond is, in fact, slightly elongated to 1.010 Å with respect to the 0.980 Å of the free acetic acid molecule.

The hydrogen−surface distances are about 2.0 Å on both surface alloys, indicating that this adsorption state should also facilitate hydrogen abstraction from acetic acid, leading to the formation of surface acetate species.

The contributions to the adsorbate−surface bonds in the η^1-$(O_C)_{cc\|}$ and η^1-$(O_H)_{cc\|}$ surface species are the weak interactions between the Pd surface atom and the sp^2 and sp^3 oxygen lone pairs of carbonyl and hydroxyl oxygen atoms, respectively. Indeed, on both PdAu surface alloys the binding energies of η^1-$(O_C)_{cc\|}$ and η^1-$(O_H)_{cc\|}$ adsorption states are 2−3 kcal/mol lower than the BEs of η^1-$(O_C)_{cc\perp}$, suggesting that the hydrogen−surface bond in the latter geometry has this strength. The η^1-$(O_H)_{cc\perp}$-CH_3COOH is not stable on the surface alloys because in this adsorption geometry the acetic acid molecule is forced in its *cis* isomeric configuration.

Let us compare now the calculated vibrational spectra of the stable η^1-CH_3COOH adsorption states with the RAIRS spectra collected from the adsorption of acetic acid on the Au-rich PdAu(111) surface alloys[31] and with the gas-phase free molecule vibrations, see Table 3.

First, in the experimental RAIRS spectra[31] two main features appear at 1720 and 923 cm^{-1} corresponding to the carbonyl C−O stretching, denoted as ν(C═O), and the hydroxyl group bending motions, denoted as γ(OH), respectively. The calculated ν(C═O) frequencies for both the η^1-$(O_C)_{cc\|}$ and the η^1-$(O_H)_{cc\perp}$ adsorption states show strong intensities at 1697−1727 cm^{-1}, in accordance with the observed experimental features. On the contrary, for η^1-(O_H)-CH_3COOH the carbonyl C−O stretching is almost 100 cm^{-1} blue shifted (1817 cm^{-1}), becoming very similar to the ν(C═O) in the free acetic acid molecule (1820 cm^{-1}).

On the other hand, the calculated γ(OH) bending frequencies of all the stable η^1-CH_3COOH adsorption states are close to those of gas-phase acetic acid (at 1184 cm^{-1}) and therefore far away from the experimentally observed features between 923 and 958 cm^{-1}. This result comes as no surprise since the RAIRS peaks in this spectral region are exclusively due to the presence of catemeric and dimeric acetic acid species that form on PdAu(111) surface alloy at the considered acetic acid coverage (i.e., 1.2 L). Although it is not the aim of the present paper to follow the variation of the vibrational frequencies of acetic acid due to formation of dimeric or catemeric species, we carried out a test calculation on the acetic acid dimer on the PdAu(111) surface. The calculated γ(OH) bending frequency for one of the possible acetic acid dimer configurations is 942 cm^{-1}, which falls in the range of the experimental values.

Moreover, the C−O_H stretching and the symmetric deformation of the CH_3 group, denoted as ν (C−O) and $\delta_s(CH_3)$, respectively, appear as broad RAIRS peaks at 1294 and 1426 cm^{-1}, and this is in good agreement with the calculated spectra. For all the adsorption states, in fact, these two vibrational modes have medium intensities and are strongly coupled in a wide frequency range between 1267 and 1435 cm^{-1}.

Finally, the stretching mode of the hydroxyl group, ν(O−H), has not been observed in the RAIRS spectra collected for the PdAu(111) surface alloy, while in the HREELS spectra of acetic acid adsorbed on Pd(111) surface[62] a broad peak at 2525 cm^{-1} has been assigned to this stretching mode. The large frequency shift of this mode with respect to the gas-phase acetic acid molecule (calculated at 3622 cm^{-1}) has been suggested to be indicative of the formation of catemers on the clean Pd surface. In the calculated vibrational spectra, as expected, this large frequency shift is not observed. The ν(O−H) vibrations lie at about 3610 cm^{-1} for the η^1-$(O_C)_{cc\|}$ and the η^1-$(O_H)_{cc\|}$ surface species. For the η^1-$(O_H)_{cc\perp}$-CH_3COOH, where a weak hydrogen bond is involved, a significant red shift has been observed in the 3243−3250 cm^{-1} range.

The theoretical cluster model results, therefore, confirm the RAIRS assignments of the ν(C═O), ν(C−O), and $\delta_s(CH_3)$ modes and support the indication of acetic acid catemers formation on PdAu surface alloys because surface acetic acid monomers do not show essential features at 920−960 and ca. 2525 cm^{-1} corresponding to the hydroxyl γ(OH) and ν(O−H) vibrational modes, respectively.

3.4. Adsorption of Acetate. The surface chemistry of acetic acid has been studied on a number of single-crystal surfaces including Pd(111),[58] Pd(110),[63] and clean and oxygen-covered Pd(100)[59] and Pd−Au alloys.[25,29,31] These experiments have indicated that acetate surface species are easily formed, even at room temperature, after acetic acid adsorption on the Pd and PdAu surfaces. Both mono- and bi-dentate spectroscopically detected acetate surface species can decompose to form CO and CO_2 or rehydrogenate to give acetic acid again. The role of Au addition to Pd surfaces is to stabilize the adsorbed acetic acid and acetate surface species by decreasing their decomposition tendency.

Theoretical studies combined with LEED measurements have shown that the preferred adsorption mode of acetate on Pd(111) surface is the bidentate species di-σ-bonded to two Pd atoms on a bridge site having the C−C axis perpendicular to the surface.[64] Binding energies of 50.7 and 52.6 kcal/mol have been calculated by use of cluster and slab supercell models, respectively.[60]

Periodic slab supercell calculations performed on second-neighbor Pd monomer pairs of PdAu(001)[34] surface alloy have shown that the preferred adsorption mode of the acetate is the di-σ-bonded on the PdAu bridge site, denoted as η^2-(O,O), having a BE equal to 47.5 kcal/mol. The π-bonded geometry, with both oxygen atoms bonded to Pd monomer in a bidentate chelating fashion, is less stable by about 13 kcal/mol.

According to these slab supercell calculations, metastable states with chelating geometry that lie approximately 11−12 kcal/mol higher in energy than the corresponding bridge adsorptions have been found on both PdAu(111) and PdAu(100) surfaces by use of cluster models. However, they

Table 4. BSSE-Corrected Binding Energies (BE, in kcal/mol), Equilibrium Bond Distances (*d*, in Angstroms), and Scaled Vibrational Frequencies (in cm^{-1}) of the η^1- and η^2-Acetate on the Pd_2Au_{55}(24,21,12) and Pd_2Au_{62}(30,21,13) Cluster Models[a]

	adsorption mode	BE	d(Pd−O_1)	d(Au−O_2)	d(C−C)	d(C−O_1)	d(C−O_2)
PdAu(100)	η^2-(O,O)	46.4	2.135	2.271	1.523	1.273	1.271
	η^1-(O)	30.5	2.114		1.514	1.321	1.234
slab supercell[b]	η^2-(O,O)	47,5	2.134	2.243			
PdAu(111)	η^2-(O,O)	34.1	2.145	2.356	1.525	1.281	1.265
	η^1-(O)	16.6	2.128		1.512	1.314	1.238

	adsorption mode	ν_{as}(OCO)	ν_s(OCO)	δ_{as}(CH_3)
PdAu(100)	η^2-(O,O)	1482 (m) +24]	1327 (s) [-5]	1417−1437 (m) [+4]
	η^1-(O)	1613 (s)	1210 (w)	1403−1425(m)
PdAu(111)	η^2-(O,O)	1480 (w) [+23]	1315 (s) [−2]	1421−1439 (w) [+4]
	η^1-(O)	1597 (s)	1232 (w)	1410−1434 (m)
PdAu(111) RAIRS[c]	η^2-(O,O)		∼1402(s)	
	η^1-(O)	∼1653 (s)		1426 (s)
PdAu(111) HREELS[d]	η^2-(O,O)	1420(br)		

[a] Differences between negatively charged ($q = -1$) and neutral acetate/cluster systems are reported in brackets. (s) strong; (m) medium; (w) weak; (br) broad. ν_{as} asymmetric stretching; ν_s symmetric stretching; δ deformation; γ bending; ρ rocking modes. [b] Reference 34. [c] Reference 31. [d] References 25 and 29.

do not result as stable local minima because they easily relax to the more stable PdAu-bridge site geometries.

Since the η^1-acetate, which can be spectroscopically distinguished from the bidentate η^2-species, has been experimentally observed to be a stable surface species, the monodentate adsorption mode, denoted as η^1-(O), has also been considered in this study. The adsorption properties, including binding energies, geometrical parameters, and vibrational frequencies, of both bidentate and monodentate modes are listed in Table 4.

It is necessary to underline that the acetate molecule has two stable rotamers having one of the HCC planes perpendicular (staggered) or parallel (eclipsed) to the OCO plane. As already shown for the adsorption of acetate on Au[65] and Ag[66] surfaces, the internal rotation of methyl group has a marginal influence on the calculated vibrational spectra. Therefore, only the more stable staggered isomer has been considered in this study.

η^2-(O,O) is strongly bonded to the palladium−gold surface alloys with binding energies of 46.4 and 34.1 kcal/mol for PdAu(100) and PdAu(111), respectively. The former BE value is in very good agreement with the previous calculated BE on PdAu(100) by the slab supercell approach,[34] while the lower BE value for the more dense PdAu(111) surface is in line with the results obtained for the other adsorbates studied here. According to the decrease of the binding energy, the Pd−O and Au−O distances increase from 2.135 to 2.145 Å and 2.271 to 2.356 Å for the PdAu(100) and the PdAu(111) surfaces, respectively.

The BE differences between the η^2-(O,O) bridge and the η^1-(O) on top adsorptions are around 16−18 kcal/mol, indicating that monodentate acetate is significantly less stable than the bidentate one on PdAu surface alloys. The only stable monodentate adsorption state has the C−C axis parallel to the surface plane.

Despite this trend in BE, shorter Pd−O bond lengths have been observed in the η^1-(O)-acetate (2.114 and 2.128 Å for the PdAu(100) and PdAu(111), respectively) with respect to the η^2-(O,O)-acetate (2.135 and 2.145 Å, respectively). These results suggest that the Au−O bond provides an important contribution to the chemisorption bond of the bidentate surface species. This argument is important since the bidentate adsorbed acetate is a key surface species in the VAM synthesis on PdAu surfaces.[25] The presence of the Au−O bond in the adsorbed surface acetate can offer further (or different) explanations for the promotional role of gold in these Pd-based catalysts and for the different reactivity observed on PdAu(100) and PdAu(111) surfaces. Indeed, the breaking of the Au−O bond instead of the Pd−O bond in the ethylene−acetate coupling reaction on PdAu(001) has been indicated as the primary motivation of the higher reactivity of second-neighbor Pd pairs with respect to contiguous Pd ensembles.[34]

Let us consider now the calculated vibrational spectra of the bidentate and monodentate acetate surface species that can be compared with previous RAIRS[31] and HREELS[25,29] experiments. The major infrared features for the surface acetate species that generally allow distinguishing between bidentate and monodentate species are the symmetric and asymmetric stretching frequencies of the carboxylic group, namely, ν_s(OCO) and ν_{as}(OCO), and the asymmetric deformations of the CH_3 group, i.e., δ_{as}(CH_3).

In the RAIRS experiments the bidentate acetate has been recognized following the ν_s(OCO) symmetric stretching feature at about 1400 cm^{-1}, whereas in the HREELS spectra a broader peak centered at 1420 cm^{-1}, assigned to the coupled (OCO) stretching frequencies and CH_3 deformation modes, has been observed. This difference can be ascribed to the compositions of the surface alloys in these experiments, namely, Pd-rich surfaces in RAIRS (the η^2-acetate is detected only at a Au mole fraction < 0.33)[31] and isolated Pd sites in HREELS.[25,29]

The calculated ν_s(OCO) stretching frequencies on PdAu surfaces are shifted to lower frequencies, at 1315−1327 cm^{-1}, with respect to the experimental features for bidentate acetate, at about 1400 cm^{-1}. On both clean Pd surfaces[58] and Pd-rich PdAu alloys[31] as well as on clean Au surfaces[65] the observed and calculated ν_s(OCO) stretching frequencies

lie at about 1400 cm^{-1}. The difference between the asymmetric di-σ bonds on the Pd−Au bridge site (see Pd−O and Au−O distances in Table 4) and the symmetrical di-σ bonds on the homonuclear Pd−Pd and Au−Au bridge sites can explain this discrepancy. In fact, the calculated ν_s(OCO) at 1315−1327 cm^{-1}, the $\delta_{as}(CH_3)$ in the 1417−1439 cm^{-1} frequency range, and the ν_{as}(OCO) at about 1480 cm^{-1} (see Table 4) are in good agreement with the broad HREELS band of the "ν (OCO) + $\delta(CH_3)$" modes, centered at 1420 cm^{-1}, observed for the Pd isolated sites.[25,29]

The formation of monodentate acetate on PdAu(111) has been recognized by RAIRS experiments[31] by means of two features at 1653 and 1426 cm^{-1} assigned to the asymmetric ν_{as}(OCO) stretching and the asymmetric methyl deformation $\delta_{as}(CH_3)$, respectively.

In accordance with Tysoe et al.[31] we found that in the monodentate adsorption mode the C−C axis is parallel to the surface plane. Indeed, the asymmetric CH_3 deformation modes lie at 1403−1434 cm^{-1} (about 1426 cm^{-1} in the RAIRS experiments), whereas the symmetric $\delta_s(CH_3)$ deformations are very weak and lie at about 1350 cm^{-1}.

The ν_{as}(OCO) stretching frequencies in the η^1-acetate become strong in intensity and blue shifted to 1597−1613 cm^{-1} with respect to those of the bidentate acetate.

For the most stable η^2-(O,O) adsorption states on PdAu(100) and PdAu(111) surfaces, both the radical and anionic acetate species have been considered in order to evaluate the effect of surface acetate species discharge on the vibrational properties. As already obtained for acetate adsorption on gold[65] and silver[66] surfaces the frequency shifts due to the cluster charge variation are small for the ν_s(OCO) stretching frequencies (∼20 cm^{-1}) and negligible for the $\delta_{as}(CH_3)$ modes (2−5 cm^{-1}).

4. Conclusions

In this work we studied the adsorption properties of ethylene, vinyl, acetic acid, and acetate species on the PdAu(111) and PdAu(100) surface alloys by the density functional cluster model approach. In particular, cluster models have been built up to represent second-neighbor Pd pairs on both surfaces since these are the critical Pd ensembles in the vinyl acetate monomer synthesis, which involves the surface species under study.

In accordance with experimental evidence and previous slab supercell calculations, our cluster model study has shown that ethylene is π bonded on Pd monomers, whereas acetate adsorbs in a bidentate fashion on a palladium−gold bridge site.

The presence of a gold−oxygen bond in the adsorbed surface acetate is confirmed by our cluster model results and should stimulate further rationalizations of the promotional role of gold in the PdAu-catalyzed VAM synthesis.

The calculated binding energies for ethylene and acetate are in very good agreement with preceding slab supercell calculations on the PdAu(100) surface, and the calculated vibrational spectra confirm the experimental frequency assignments, giving more details regarding all the involved vibrational modes.

Even if the surface vinyl species has not been detected on PdAu surface alloys, theoretical predictions on the adsorption properties of the vinyl radical on second-neighbor Pd pairs have been reported in order to be possibly compared with future experimental studies. The surface vinyl species has shown, in fact, strong interactions with Pd monomers and also with Au surface atoms. The calculated vibrational spectra are quite different from those of the adsorbed ethylene molecules.

Density functional cluster model results on the adsorption of acetic acid monomers have confirmed the experimental assignments of the major vibrational modes in the infrared spectra, supporting the indication that acetic acid catemers form on PdAu surface alloys. However, at very low acetic acid coverages, monomeric species should be present on PdAu surfaces, and our results suggest that it adsorbs in a monodentate fashion, forming a weak hydrogen bond with the surface.

In general, the adsorption of all molecules on the bimetallic PdAu surfaces is a less efficient process with respect to the clean Pd surfaces. The ligand effect of the gold atoms surrounding the Pd monomers lowers the adsorption energies. This effect is more pronounced for the more dense PdAu(111) surface alloy.

Finally, the adopted cluster models have been demonstrated to be sufficiently reliable by giving accurate results on the adsorption properties, including binding energies, preferred adsorption sites, stable bonding modes, geometrical parameters, and vibrational frequencies, in full agreement with available slab supercell calculations and the experimental evidence.

Acknowledgment. The authors thank the Università della Calabria for financial support.

References

(1) Sinfelt, J. H. *Bimetallic Catalysts: Discoveries, Concepts and Applications*; Wiley: New York, 1983.

(2) Somorjai, G. *Introduction to Surface Chemistry and Catalysis*; John Wiley & Sons: New York, 1994.

(3) Rodriguez, J. A. *Surf. Sci. Rep.* **1996**, *24*, 223–287.

(4) Moss, R. L.; Whally, L., *Advances in Catalysis*; Academic Press: New York, 1972.

(5) Baddeley, C. J.; Tikhov, M.; Hardacre, C.; Lomas, J. R.; Lambert, R. M. *J. Phys. Chem.* **1996**, *100*, 2189–2194.

(6) Baddeley, C. J.; Ormerod, R. M.; Stephenson, A. W.; Lambert, R. M. *J. Phys. Chem.* **1995**, *99*, 5146–5151.

(7) Han, Y. F.; Kumar, D.; Goodman, D. W. *J. Catal.* **2005**, *230*, 353–358.

(8) Enache, D. I.; Edwards, J. K.; Landon, P.; Solsona-Espriu, B.; Carley, A. F.; et al. *Science* **2006**, *311*, 362–365.

(9) Trimm, D. L.; Önsan, Z. I. *Catal. Rev.* **2001**, *43*, 31–84.

(10) Bonarowska, M.; Malinowski, A.; Juszczyk, W.; Karpinski, Z. *Appl. Catal., B* **2001**, *30*, 187–193.

(11) Li, Z.; Gao, F.; Wang, Y.; Calaza, F.; Burkholder, L.; Tysoe, W. T. *Surf. Sci.* **2007**, *601*, 1898–1908.

(12) Yi, C. W.; Luo, K.; Wei, T.; Goodman, D. W. *J. Phys. Chem. B* **2005**, *109*, 18535–18540.

(13) Legawiec-Jarzyna, M.; Srebowata, A.; Karpinski, Z. *React. Kinet. Catal. Lett.* **2003**, *79*, 157–161.

(14) Venezia, A. M.; La Parola, V.; Pawelec, B.; Fierro, J. L. G. *Appl. Catal., A* **2004**, *264*, 43–51.

(15) Maroun, F.; Ozanam, F.; Magnussen, O. M.; Behm, R. J. *Science* **2001**, *293*, 1811–1814.

(16) Sarkany, A.; Horvath, A.; Beck, A. *Appl. Catal., A* **2002**, *229*, 117–125.

(17) Hilaire, L.; Legare, P.; Holl, Y.; Maire, G. *Surf. Sci.* **1981**, *103*, 125–140.

(18) Jablonski, A.; Overbury, S. H.; Somorjai, G. A. *Surf. Sci.* **1977**, *65*, 578–592.

(19) Provine, W. D.; Mills, P.; Lerov, J. J. *Stud. Surf. Sci. Catal.* **1996**, *101*, 191–200.

(20) Samanos, B.; Boutry, P.; Montarnal, R. *J. Catal.* **1971**, *23*, 19–30.

(21) Moiseev, I.; Vargaftic, M. N.; Syrkin, Y. L. *Dokl. Akad. Nauk SSSR* **1960**, *133*, 377–380.

(22) Moiseev, I. *Catalytic Oxidation*; Sheldon, R. A., Ed.; World Scientific, 1995; p 203.

(23) Nakamura, S.; Yasui, T. *J. Catal.* **1970**, *17*, 366–374.

(24) Stacchiola, D.; Calaza, F.; Burkholder, L.; Tysoe, W. T. *J. Am. Chem. Soc.* **2004**, *126*, 15384–15385.

(25) Chen, M.; Kumar, D.; Yi, C. W.; Goodman, D. W. *Science* **2005**, *310*, 291–293, including supporting online material.

(26) Han, P.; Axnanda, S.; Lyubinetsky, I.; Goodman, D. W. *J. Am. Chem. Soc.* **2007**, *129*, 14355–14361.

(27) Luo, K.; Wei, T.; Yi, C. W.; Axnanda, S.; Goodman, D. W. *J. Phys. Chem. B* **2005**, *109*, 23517–23522.

(28) Calaza, F.; Gao, F.; Li, Z.; Tysoe, W. T. *Surf. Sci.* **2007**, *601*, 714–722.

(29) Chen, M. S.; Luo, K.; Wei, Z.; Yan, Z.; Kumar, D.; Yi, C. W.; Goodman, D. W. *Catal. Today* **2006**, *117*, 37–45.

(30) Owens, T. G.; Jones, T. E.; Noakes, T. C. Q.; Bailey, P.; Baddeley, C. J. *J. Phys. Chem. B* **2006**, *110*, 21152–21160.

(31) Calaza, F.; Gao, F.; I, Z; Tysoe, W. T. *Surf. Sci.* **2007**, *601*, 1351–1357.

(32) García-Mota, M.; Lopez, N. *J. Am. Chem. Soc.* **2008**, *130*, 14406–14407.

(33) Yuan, D.; Gong, X.; Wu, R. *Phys. Rev. B* **2007**, *75*, 233401–233404.

(34) Yuan, D.; Gong, X.; Wu, R. *J. Phys. Chem. C* **2008**, *112*, 1539–1543.

(35) Mazzone, G.; Rivalta, I.; Russo, N.; Sicilia, E. *J. Phys. Chem. C* **2008**, *112*, 6073–6081.

(36) Ahlrichs, R.; Bär, M.; Häser, M.; Horn, H.; Kölmel, C. *Chem. Phys. Lett.* **1989**, *162*, 165–169.

(37) Becke, A. D. *Phys. Rev. A* **1988**, *38*, 3098–3100.

(38) Perdew, J. P. *Phys. Rev. B* **1986**, *33*, 8822–8824.

(39) Eichkorn, K.; Treutler, O.; Öhm, H.; Häser, M.; Ahlrichs, R. *Chem. Phys. Lett.* **1995**, *240*, 283–289.

(40) Eichkorn, K.; Weigend, F.; Treutler, O.; Ahlrichs, R. *Theor. Chem. Acc.* **1997**, *97*, 119–124.

(41) Andrae, D.; Hæussermann, U.; Dolg, M.; Stoll, H.; Preuss, H. *Theor. Chim. Acta* **1990**, *77*, 123–141.

(42) Schäfer, A.; Huber, C.; Ahlrichs, R. *J. Chem. Phys.* **1994**, *100*, 5829–5835.

(43) Boys, S. F.; Bernardi, F. *Mol. Phys.* **1970**, *19*, 553–566.

(44) Neugebauer, J.; Hess, B. A. *J. Chem. Phys.* **2003**, *118*, 7215–7225.

(45) Ge, Q.; Neurock, M. *Chem. Phys. Lett.* **2002**, *358*, 377–382.

(46) Neurock, M.; van Santen, R. A. *J. Phys. Chem. B* **2000**, *104*, 11127–11145.

(47) Mei, D.; Hansen, E. W.; Neurock, M. *J. Phys. Chem. B* **2003**, *107*, 798–810.

(48) Yuan, D.; Gong, X.; Wu, R. *Phys. Rev. B* **2007**, *75*, 085428−085432.

(49) Dewar, M. J. S. *Bull. Soc. Chim. Fr.* **1951**, *18*, C71−C79.

(50) Chatt, J.; Duncanson, L. A. *J. Chem. Soc.* **1953**, *75*, 2939–2947.

(51) Masel, R. I. *Principles of Adsorption and Reaction on Solid Surfaces*; John Wiley and Sons: New York, 1996.

(52) Yagasaki, E.; Masel, R. *Catalysis* **1994**, *11*, 165–222.

(53) Stuve, E. M.; Madix, R. J. *J. Phys. Chem.* **1985**, *89*, 105–112.

(54) Zaera, F.; Hall, R. B. *Surf. Sci.* **1987**, *180*, 1–18.

(55) Pallassana, V.; Neurock, M.; Lusvardi, V. S.; Lerou, J. J.; Kragten, D. D.; van Santen, R. A. *J. Phys. Chem. B* **2002**, *106*, 1656–1669.

(56) Azad, S.; Kaltchev, M.; Stacchiola, D.; Wu, G.; Tysoe, W. T. *J. Phys. Chem. B* **2000**, *104*, 3107–3115.

(57) Stacchiola, D.; Calaza, F.; Zheng, T.; Tysoe, W. T. *J. Mol. Catal A: Chem.* **2005**, *228*, 35–45.

(58) Haley, R. D.; Tikhov, M. S.; Lambert, R. M. *Catal. Lett.* **2001**, *76*, 125–130.

(59) Li, Z.; Gao, F.; Tysoe, W. T. *Surf. Sci.* **2008**, *602*, 416–423.

(60) Pallassana, V.; Neurock, M. *J. Catal.* **2002**, *209*, 289–305.

(61) Burneau, A.; Génin, F.; Quilès, F. *Phys. Chem. Chem. Phys.* **2000**, *2*, 5020–5029.

(62) Davis, J. L.; Barteau, M. A. *Langmuir* **1989**, *5*, 1299–1309.

(63) Bowker, M.; Morgan, C.; Couves, J. *Surf. Sci.* **2004**, *555*, 145–156.

(64) James, J.; Saldin, D. K.; Zheng, T.; Tysoe, W. T.; Sholl, D. S. *Catal. Today* **2005**, *105*, 74–77.

(65) Bernà, A.; Delgado, J. M.; Orts, J. M.; Rodes, A.; Feliu, J. M. *Electrochim. Acta* **2008**, *53*, 2309–2321.

(66) Delgado, J. M.; Rodes, A.; Orts, J. M. *J. Phys. Chem. C* **2007**, *111*, 14476–14483.

CT9000137